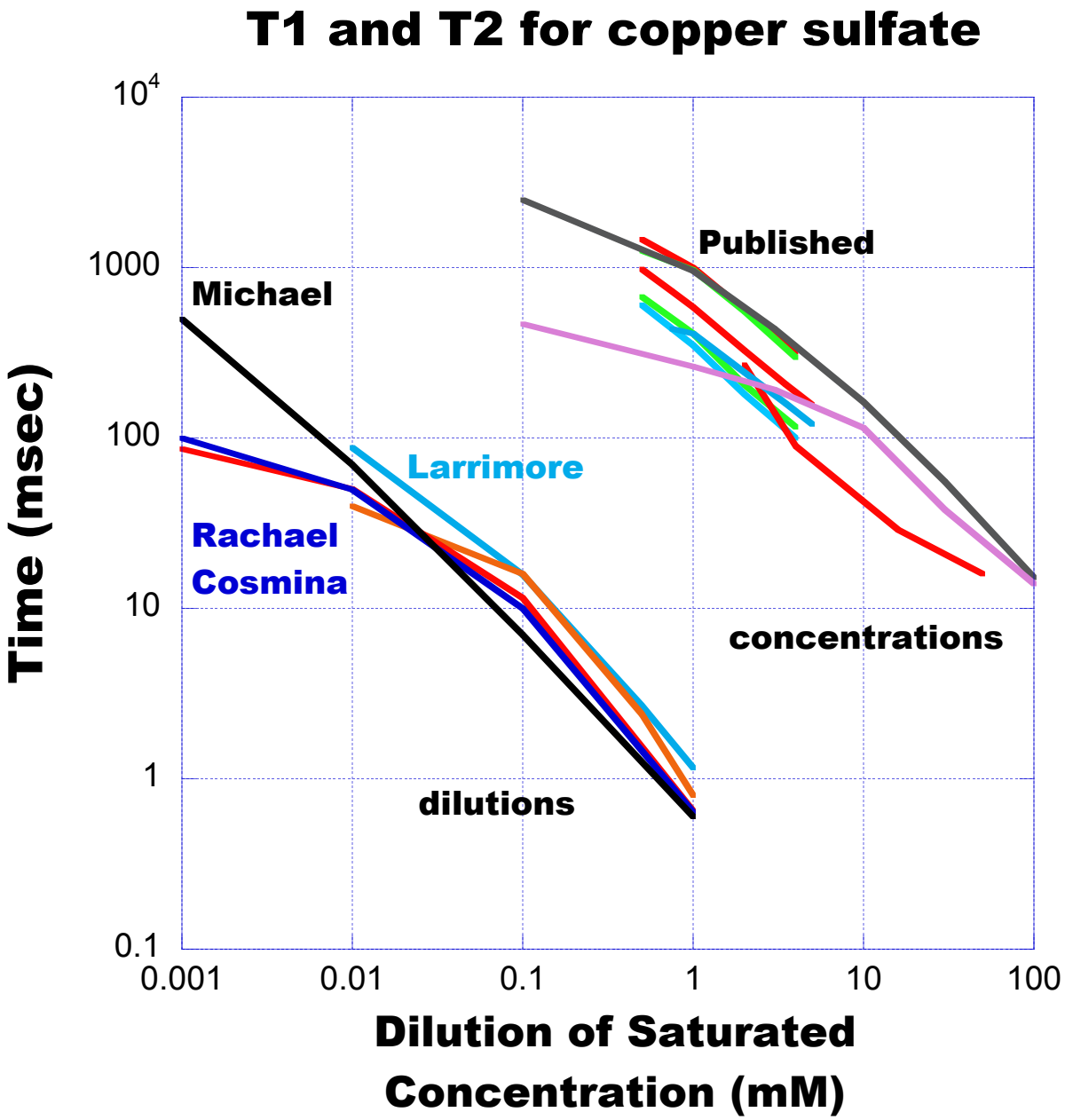
T1 and T2 for copper sulfate
Time (msec)
10^4
1000
100
10
1
0.1
0.001
0.01
0.1
1
10
100
Dilution of Saturated Concentration (mM)
Published
Michael
Larrimore
Rachael
Cosmina
concentrations
dilutions

8.1 Relaxation in NMR Spectroscopy

An understanding of relaxation processes is important for the proper measurement and interpretation of NMR spectra. There are three important considerations.

1. The very small energy difference between α and β states of a nuclear spin orientation in a magnetic field results in a very small excess population of nuclei in the ground vs the excited states. For many nuclei relaxation (i.e., return from excited to ground state) is a very slow process, with half-lives on the order of 0.1 to 100 seconds for a spin ½ nucleus (compare this with micro-, pico- and femtoseconds for relaxation of electronic and vibrational transitions). It is thus very easy to *saturate* an NMR transition (equalize populations of excited and ground state), with the resultant loss in signal quality, and failure to obtain correct peak areas.

2. NMR lines are extraordinarily sharp, and extraordinarily close together (in energetic terms) compared to other spectroscopic methods. So much so that Heisenberg uncertainty broadening (which is a function of lifetime of a given energy state, and hence relaxation rates) is a dominant feature of many NMR spectra, and can limit our ability to measure and interpret spectra. When relaxation is very fast, NMR lines are broad, *J*-coupling may not be resolved or the signal may even be difficult or impossible to detect.

3. The success of many multipulse experiments, especially 2D and 3D spectra, depends crucially on proper consideration of relaxation times.

T_1 and T_2 Relaxation. We distinguish two types of relaxation, *Spin-Lattice* (T_1, also known as longitudinal relaxation, or relaxation in the z-direction) and *Spin-Spin* (T_2, also known as transverse relaxation, or relaxation in the x-y plane). T_1 relaxation corresponds to the process of establishing (or re-establishing) the normal Gaussian population distribution of α and β spin states in the magnetic field. T_2 is loss of phase coherence among nuclei. T_2 is less than or equal to T_1 (T_2 relaxation is the same as or faster than T_1 relaxation, R = relaxation rate, $R_2 = 1/T_2$, $R_2 \geq R_1$), since return of magnetization to the z-direction inherently causes loss of magnetization in the x-y plane. The line width of an NMR signal is determined by T_2 (short T_2 means broader lines, $\nu_{1/2} = 1/\pi T_2$, $\nu_{1/2}$ = width at half height), the maximum repetition rate during acquisition of an NMR signal is governed by T_1 (short T_1 means signal can be acquired faster).

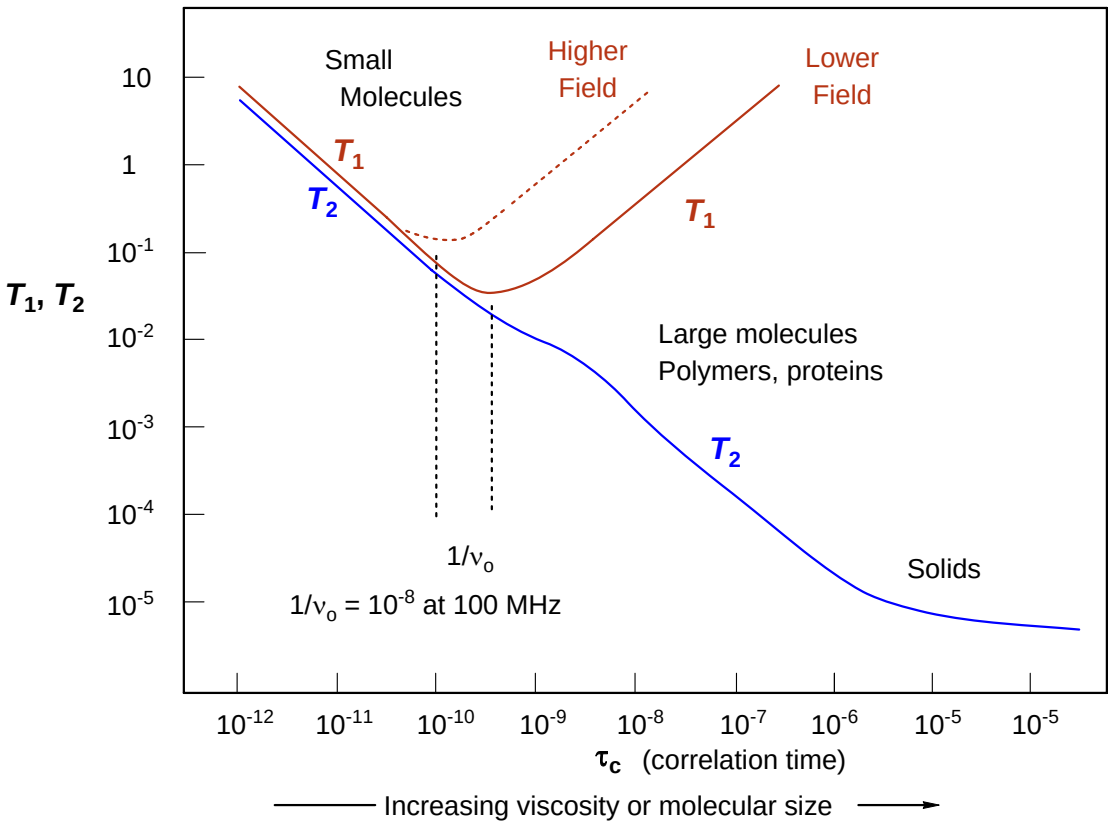

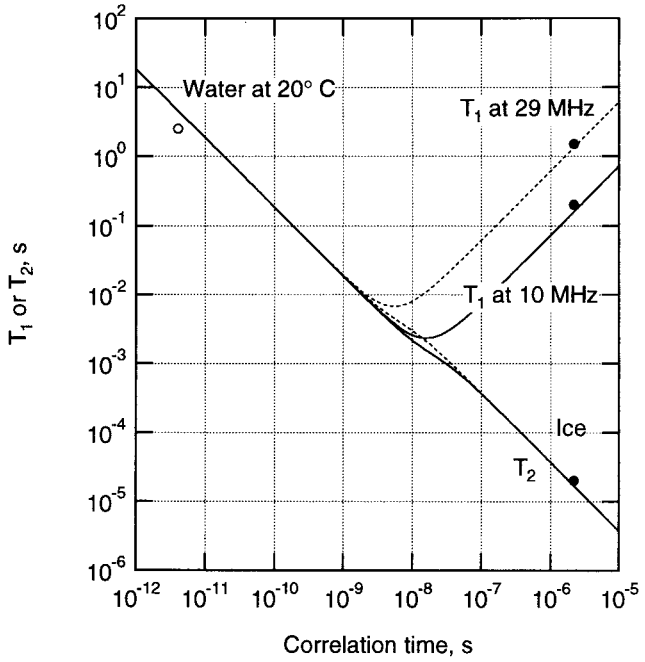

FIGURE 17.12. Plot of T_1 and T_2 vs correlation time of the fluctuating magnetic field at the nucleus. Experimental points are shown for water (open dot) and ice (solid dot).

$$\frac{1}{T_1}=\frac{C\tau_c}{1+\omega_0^2\tau_c^2}, \tag{17.33}$$

where C is the proportionality constant.

The correlation time in a solid is much longer than in a liquid. For example, in liquid water at 20 °C it is about 3.5×10^{-12} s; in ice it is about 2×10^{-6} s. Figure 17.12 shows the behavior of T_1 as a function of correlation time, plotted from Eq. (17.33) with $C=5.43\times10^{10}$ s^{-2}. For short correlation times T_1 does not depend on the Larmor frequency. At long correlation times T_1 is proportional to the Larmor frequency, as can be seen from Eq. (17.33). The minimum in T_1 occurs when $\omega_0=1/\tau_c$ in this model.

Table 17.2 shows some typical values of the relaxation times at 20 MHz. Neighboring paramagnetic atoms reduce the relaxation time by causing a fluctuating magnetic field. For example, adding 20 ppm of Fe^{3+} to water reduces T_1 to 20 ms.

Differences in relaxation time are easily detected in an image. Different tissues have different relaxation times. A contrast agent containing gadolinium is often used in magnetic resonance imaging. It is combined with many of the same pharmaceuticals used with ^{99m}Tc, and it reduces the relaxation time of nearby nuclei. The hemoglobin that carries oxygen in the blood exists in two forms: oxyhemoglobin and deoxyhemoglobin. The former is diamagnetic and the latter is paramagnetic, so the relaxation time in blood depends on the amount of oxygen in the hemoglobin. The technique that exploits this is called BOLD (blood oxygen level dependence).

TABLE 17.2. *Approximate relaxation times at 20 MHz.*

	T_1 (ms)	T_2 (ms)
Whole blood	900	200
Muscle	500	35
Fat	200	60
Water	3000	3000

It was pointed out in Sec. 17.4 that because of dephasing, T_2 is less than or equal to T_1. The same model for the fluctuating fields which led to Eq. (17.33) gives an expression for T_2:

$$\frac{1}{T_2}=\frac{C\tau_c}{2}+\frac{1}{2T_1}. \tag{17.34}$$

There is a slight frequency dependency to T_2 for values of the correlation time close to the reciprocal of the Larmor frequency.

Another effect that causes the magnetization to rapidly decrease is dephasing. Dephasing across the sample occurs because of inhomogeneities in the externally applied field. Suppose that the spread in Larmor frequency and the transverse relaxation time are related by $T_2\Delta\omega=K$. (Usually K is taken to be 2.) The spread in Larmor frequencies $\Delta\omega$ is due to a spread in magnetic field ΔB experienced by the nuclear spins in different atoms. The total variation in B is due to fluctuations caused by the magnetic field of neighbors and to variation in the applied magnetic field across the sample:

$$\Delta B_{\text{tot}}=\Delta B_{\text{internal}}+\Delta B_{\text{external}}.$$

Therefore

$$\Delta\omega_{\text{tot}}=\Delta\omega_{\text{internal}}+\Delta\omega_{\text{external}}.$$

The total spread is associated with the experimental relaxation time, $T_2^*=K/\Delta\omega_{\text{tot}}$. The "true" or "non-recoverable" relaxation time $T_2=K/\Delta\omega_{\text{internal}}$ is due to the fluctuations in the magnetic field intrinsic to the sample. Therefore

$$\frac{1}{T_2^*}=\frac{1}{T_2}+\frac{\gamma\Delta B_{\text{external}}}{K}. \tag{17.35}$$

T_2 is called the *nonrecoverable* relaxation time because various experimental techniques can be used to compensate for the external inhomogeneities, but not the atomic ones.

17.7. DETECTING THE SIGNAL

We have now seen that a sample of nuclear spins in a strong magnetic field has an induced magnetic moment, that it is possible to apply a sinusoidally varying magnetic field and nutate the magnetic moment to precess at any arbitrary

Relationship between T_1 and T_2

Simple, small molecule:

Fast, tumbling liquid
Narrow lines

Rigid, frozen solid
Broad lines

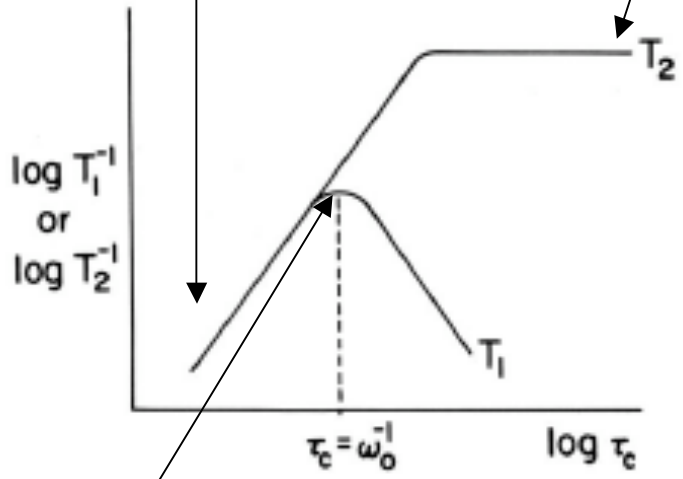

τ_c refers to the correlation time of tumbling
Close to the inflection point, experiments can be done quickly

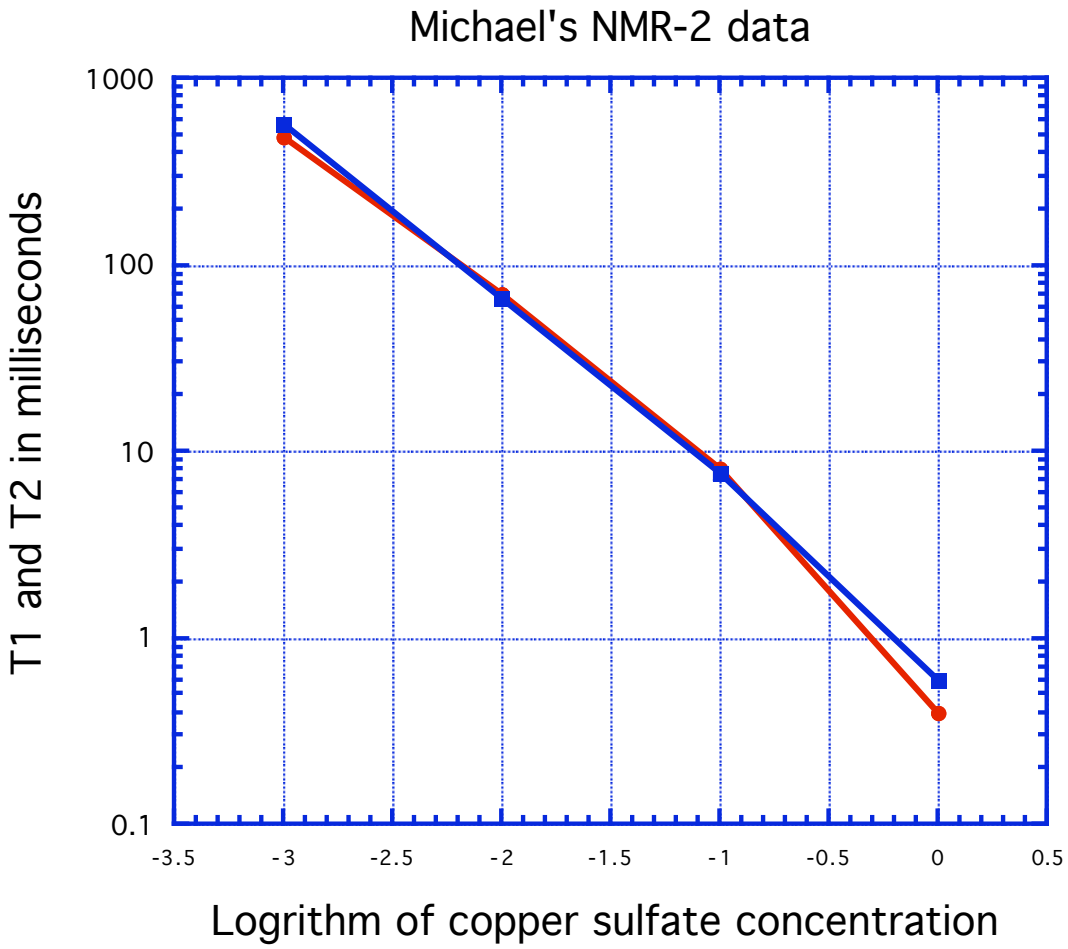
Michael's NMR-2 data
T1 and T2 in milliseconds
1000
100
10
1
0.1
-3.5
-3
-2.5
-2
-1.5
-1
-0.5
0
0.5
Logrithm of copper sulfate concentration

MHz. Using these measurements, Eq. (11) shows that the magnetic moment of the proton is

$$\mu_p = \frac{\omega_0 \hbar}{2B_0} = 1.414 \times 10^{-26} \text{J/T}. \tag{15}$$

This is 0.2% different from the theoretical value given in Eq. (3), which is exactly the percent error in our measurements.

Figure (2) shows the data taken to measure T_1 for the mineral oil sample. The spin-lattice relaxation time was determined to be $T_1 = 60.0 \pm 0.3$ ms by fitting the data to an exponential function going from $-M_0$ to M_0. Figure (3) shows the data taken to measure T_2 for the mineral oil sample. The spin-spin relaxation time was determined to be $T_2 = 57 \pm 1$ ms by an exponential fit.

The measurements of T_1 for the various concentrations of $CuS0_4$ in distilled water are shown in Figures (4-7), and the measurements of T_2 are shown in Figures (8-11). A summary of these relaxation times is shown in Table (1).

Table 1: Relaxation times T_1 and T_2 for $CuSO_4$ solutions

relative concentration	T_1 (ms)	T_2 (ms)
1%	87.6 ± 0.6	40 ± 1
10%	15.8 ± 0.1	16.0 ± 0.5
50%	2.71 ± 0.05	2.4 ± 0.1
100%	1.16 ± 0.02	0.80 ± 0.03

When the inverse of the relaxation times is plotted versus the relative concentration of $CuSO_4$, the data can be fit with a quadratic function, as in Figure (12). While the exact nature of the relationship between concentration and relaxation time is unclear, it is clear that higher concentrations of $CuSO_4$ decrease the relaxation time of the protons in distilled water. Futhermore, as expected, T_2 is greater than T_1 for all solutions (except the 10% solution, for which the difference is less than their absolute errors). The fact that the difference between the two relaxation times is generally small means that the additional factor for T_2, the dephasing due to spin interactions, is not as significant as the realignment of protons with the constant magnetic field.

vided T_2 is replaced by T_2^*, the time for the free induction signal to de-phase in the residual gradients of the static field. For multi-echo (ME) sequences the ratio of the signal from a late echo at $T_{E'}$ to that from the first echo at $T_E < T_{E'}$ is therefore given by

$$S'/S = e^{-(T_{E'}-T_E)/T_2}$$

that is the contributions to signal intensity from spin density, flip angle and T_1 divide out, being common to both echos in the same sequence. If such a division is carried out on a pixel by pixel basis then, contrast in the resulting image will depend only on T_2 (or T_2^* in the case of gradient echo images). It is not strictly a calculated T_2 image in the conventional sense because the pixel values are not linear in T_2. Compared with a simple two-point fit calculated T_2 image it requires less computation and the image contrast is more closely related to that obtained in a conventional T_2 weighted image, without the additional complication of a functional dependence on T_1 and N(H).

RESULTS AND DISCUSSION

In order to evaluate the technique it was necessary first to investigate under what conditions our imaging system was capable of yielding accurate and reproducible relaxation times. A phantom was therefore constructed comprising six plastic bottles of 250 ml capacity containing water doped with $CuSO_4$ with concentrations in the range 0.1 mM to 100 mM. Samples of these same solutions in 10 mm NMR tubes were taken in order to compare relaxation times measured on the imaging system with values obtained on a conventional NMR spectrometer. The spectrometer employed was a Bruker SXP machine operating at 60 MHz which had been extensively modified and upgraded for automated measurement of relaxation times.[7] Measurements of the spin-lattice relaxation time T_1 were made using either inversion recovery or saturation recovery sequences, while T_2 values were obtained using the Carr-Purcell spin-echo method.[8] In all cases at least twelve pulse delay times/echo times were employed to map out the relaxation and the measurements were repeated several times to check consistency. The results are summarized in Table 1.

Also shown in Table 1 are relaxation times measured on the phantom in our GE Signa imaging system operating at 63.9 MHz (1.5 T). These measurements were all made using the headcoil with a multi-echo saturation recovery imaging sequence (ME) in multi-slice imaging mode with 5 mm slice thickness and four echos at T_E values of 20, 40, 60 and 80 ms. The sequence repetition time T_R was stepped through five values between 125 and 2000 ms, giving five-point fits for the T_1 data and four point fits for T_2, a region of interest being selected from the final images in each bottle of the phantom. A comparison of T_1 values calculated from early and late echos yielded no systematic differences. Likewise T_2 values calculated from data corresponding to different T_R values agreed within experimental error. There was also no systematic dependence of relaxation times measured from center or end slices when more than one slice was imaged simultaneously, at least for slice spacings down to 1 mm. We also found no dependence of relaxation times on whether transmitter and receiver attenuation factors were set manually or using 'auto prescan.' Errors in the relaxation times for the imaging system in Table 1 represent the standard deviation of values obtained under different operating conditions and include two sets of measurements separated in time by 1 week.

Table 1. Comparison of relaxation times (in milliseconds) for $CuSO_4$ solutions measured on a Bruker SXP spectrometeer operating at 60 MHz with values obtained on a GE Signa imaging system at 63.9 MHz

$CuSO_4$ (mM)	Spectrometer		Imager	
	T_1	T_2	T_1	T_2
0.1	2501 ± 24	467 ± 39	2344 ± 340	210 ± 16
1.0	960 ± 16	263 ± 20	951 ± 80	189 ± 10
3.0	439 ± 5	193 ± 7	404 ± 21	129 ± 4
10	163 ± 2	115 ± 3	129 ± 4	80 ± 4
30	55.7 ± 0.4	38.1 ± 0.9	44.6 ± 2.0	32.8 ± 3.3
100	15.2 ± 0.2	14.0 ± 0.2	12.0 ± 0.6	12.0 ± 0.2

Comparison of the relaxation times from the imaging system with those obtained on the spectrometer indicate that the former are systematically shorter. This is also seen in Fig. 1, where the corresponding relaxation rates $(1/T_1, 1/T_2)$ are plotted against the concentration of $CuSO_4$. The solid line which approximates the spectrometer T_1 data at high concentrations corresponds to the relation

$$1/T_1 = 0.658C + 0.027$$

where C is the $CuSO_4$ concentration in mM. In the case of T_1 values the discrepancy is relatively small, although the higher frequency of the imager measurements indicates that these values should be slightly longer. Much greater differences were found in the T_2 values, particularly those in excess of 100 ms, where both spectrometer and imager measured spin-spin relaxation rates were found to deviate from a lin-

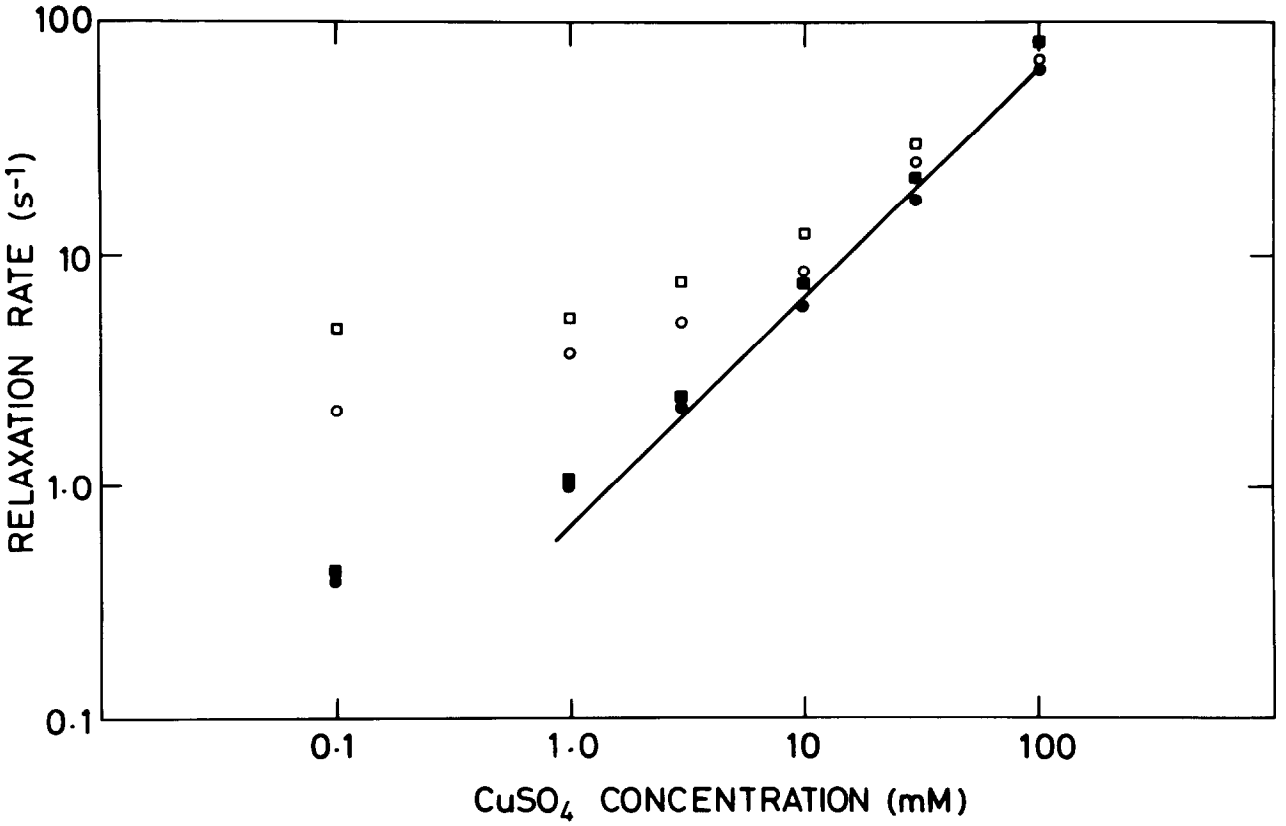

Fig. 1. Comparison of relaxation rates for water protons in solutions of $CuSO_4$ of varying concentrations measured on an imaging machine at 63.9 MHz (square symbols) with those obtained on a spectrometer at 60 MHz (circles): ● ■ $1/T_1$; ○ □ $1/T_2$.

ear dependence on paramagnetic ion concentration at low concentrations due to effects of diffusion and convection in the bulk solutions, imperfect 180° pulses and field or phase instabilities. Similar systematic differences between imager and spectrometer measured T_2 values have been reported by MacFall et al,[6] who attribute them to the effects of imperfect pulses and uncompensated eddy currents resulting from the field gradient pulses employed to provide spatial discrimination on the imaging system. Overall, however, the results confirm that the imager-measured relaxation times are reproducible to better than 10% under clinically realistic operating at conditions (multi-slice, auto-prescan, etc.) provided of course that pulse flip angles and transmitter and receiver attenuation factors are not altered during the course of the measurements. Furthermore, with the exception of the systematic deviations in T_2 values for $T_2 > 100$ ms mentioned above, the results appear surprisingly accurate.

Having demonstrated the accuracy and reliability of relaxation times measured on the imaging system, we proceeded to employ the same phantom to test our method of calculating T_2 images. In order to do this we employed the standard command line image processing system (CLIPS) software supplied by GE, which allows simple arithmetic manipulation of images on a pixel by pixel basis. The results are illustrated in Fig. 2, which shows the raw images of our phantom derived from first and last echos respectively at the top and the processed images below. The concentration of $CuSO_4$ in the bottles decreases from top left to bottom right in these images. The image at bottom left in Fig. 2 was obtained by simple division of the late echo image by the early echo one (after subtraction of an intensity offset introduced by the imaging machine and prescaling to avoid effects of integer arithmetic). Note that in both raw images, as a result of partial saturation effects, the signal intensities do not follow the order of concentrations of paramagnetic ions in the bottles, confirming that, as expected, contrast in these images is affected by T_1 as well as T_2 [Eq. (2)]. In the calculated image, in contrast, the intensities follow the order of T_2 values. This image is however marred by noise arising from regions outside the

Table 1. $T1$ Relaxation, TDC, activation energy and viscosity thermal characteristics (at 22°C and 6.25 MHz)

Sample	$T1$ (msec)	TDC (%/°C)	E_a (kcal/Mol)	Viscosity (%/°C)
$CuSO_4$				
5.0 mM	157 ± 10	2.07	2.96	−0.93
3.5 mM	207 ± 21	2.30	3.20	
2.0 mM	328 ± 38	2.52	3.42	
1.0 mM	588 ± 72	2.53	3.45	
.75 mM	727 ± 100	2.39	3.24	
.50 mM	983 ± 165	2.42	3.28	
		2.37 ± .17	3.26 ± .18	
Oils				
Corn	121 ± 10	3.63	4.35	
Sesame	123 ± 4	3.75	4.44	
Crisco	122 ± 5	3.40	4.16	−1.60
	122 ± 3	3.59 ± .18	4.32 ± .14	
Solutions				
95% ETOH	2058 ± 276	2.84	3.97	−0.74
10% Liposyn	1688 ± 205	2.71	3.38	−0.89
5% BSA	1327 ± 245	1.69	2.87	
Egg				
Yolk	84 ± 15	1.39	2.13	
White	794 ± 60	0.64	1.08	

$T1$ values (<500 ms) to approximately 10% for long $T1$ values (≥1000 ms). The uncertainties for the $T2$ values tended to be larger. A significant factor was the presence of severe banding artifacts in multi-echo studies (eddy currents being one possible explanation) that leads to large uncertainties in individual data points. In addition, the possible multi-compartment behavior mentioned earlier is also considered a contributing factor.

Temperature Dependence of Relaxation Times

The temperature was maintained to within less than 1°C of the nominal value as verified by continuous temperature recording. The $T1$ values were measured at five discrete temperature points from 20°C to 50°C (21, 28, 37, 44, 50°C) and showed a linear increase in $T1$ with temperature (Figs. 2 and 3) as predicted by Eqs. 2, 3 and 4.

A semi-log curve of relaxation time versus inverse absolute temperature ($1/T$) for copper sulfate is plotted in Fig. 4. The slope of the solid line corresponds to the activation energy, E_a as described by the FETS model. E_a was determined by fitting the data to Eq. (10) and is given in Table I for each sample. Figure 5 shows a similar semi-log curve for the samples in groups #2–#4.

Over a small temperature change the relaxation time and temperature demonstrate a linear relationship that may be approximated by:

Table 2. $T2$ Relaxation and TDC thermal characteristics (at 22°C and 6.25 MHz)

Sample	$T2$ (msec)	TDC (%/°C)
$CuSO_4$		
5.0 mM	121 ± 10	2.07
3.5 mM	160 ± 8	1.47
2.0 mM	244 ± 22	1.86
1.0 mM	411 ± 4	1.44
.75 mM	438 ± 24	1.36
		1.49 ± .22
Oils		
Corn	105 ± 5	1.69
Sesame	95 ± 5	2.04
Crisco	108 ± 7	1.25
Solutions		
95% ETOH	185 ± 15	0.09
10% Liposyn	542 ± 11	0.09
5% BSA	520 ± 15	−0.27
Egg		
Yolk	18 ± 15	−0.06
White	410 ± 20	−0.35

$$T1 = T1^\circ + A * T \tag{12}$$

where both $T1^\circ$ and A are empirical constants and T is the temperature in °C. The parameters [$T1^\circ$ and A] were determined using a linear regression fit.

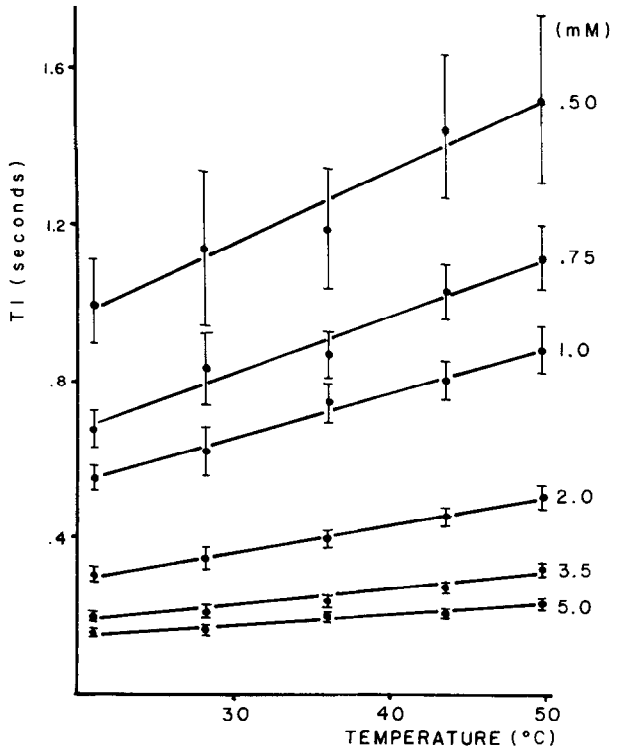

Fig. 2. A plot of the change in $T1$ versus temperature (°C) for temperatures between 20 and 50° for $CuSO_4$ solutions. Note that the relative increase in $T1$ with increasing temperature is greater for solutions with a longer $T1$ although the % increase is relatively constant as shown in the accompanying data table.

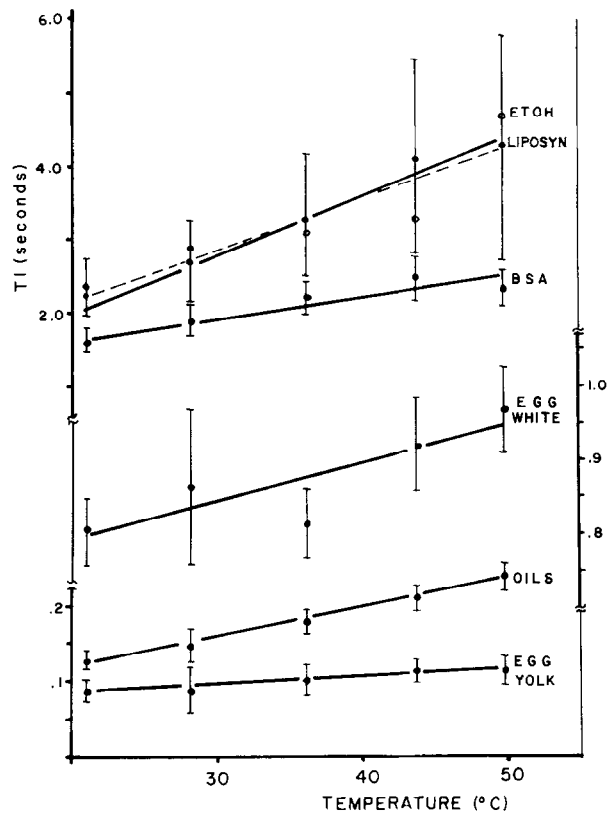

Fig. 3. A plot of the change in $T1$ versus temperature (°C) for temperatures between 20 and 50° for different samples. Note that the relative increase in $T1$ with increasing temperature depends upon the solution as well as the initial temperature.

We now define a temperature dependence coefficient (TDC) for proton relaxation times, over the range of clinically and experimentally interesting temperatures ($15° < T < 50°$), as:

$$\text{TDC} = 100\% * \frac{A}{\text{Relaxation time at reference temperature}} \tag{13}$$

where A is the constant in Eq. 12. For measurements made above freezing point of solvent, e.g. water in this study, a reference temperature of 22°C is proposed for Eq. 13. The TDC's for each sample studied are listed in Tables I and II.

The average TDC for $CuSO_4$ solutions at 22°C is 2.37%/°C. For oil samples, the TDC is 3.59 %/°C, or about 50% higher than that of $CuSO_4$. In the third group, the TDC value is different for each sample. It can be appreciated that the TDC of the tissue-simulating solutions is similar to that of the copper sulfate solutions. The TDC of the egg samples is lower than the other samples.

The TDC's of $T2$ for all investigated samples were also calculated. A relatively small TDC was found for $T2$ values. It should be noted that, for the $T2$ values of most samples, the temperature dependence is statistically non-significant. The TDC is also negative for some samples; i.e. $T2$ decreases as the temperature increases. These findings are in agreement with the previous studies.[13,21]

Temperature Dependence of Viscosity

The temperature was maintained to within ±0.2°C for all viscosity measurements. In all fluids the viscosity showed an inverse relationship with respect to temperature change. The magnitude of the change also depended on the specific fluid. The viscosity temperature coefficient is given in Table I for the fluids studied. The viscosity characteristics were also measured for pure water and did not show a significant difference from the $CuSO_4$ solutions.

ensure that the transition is complete. The hot solution is then poured into a vial or other mold and allowed to solidify into a gel. The permanent container is completely filled and sealed to prevent evaporative loss or exchange of D_2O for H_2O.

To make gels of several different copper ion concentrations from a single batch of hot agarose, the agar solution is prepared in a concentration higher than the desired final concentration. The additional water needed to reach the appropriate agarose concentration is placed in each vial, along with the desired amount of copper sulfate. The solutions must be mixed well when the hot agar is added. The agar concentration in individual gels prepared from a single batch can similarly be varied.

RELAXATION TIMES OF THE AGAROSE-COPPER SULFATE GELS

The measurements of relaxation times of the samples were carried out on an NMR spectrometer that was tuned to either 5 or 60 MHz. The T1 value was determined by using an inversion-recovery pulse sequence and measuring T-null, from which T1 is calculated. The T2 value was determined by fitting an exponential curve to the envelope of the spin echoes resulting from a Carr-Purcell-Meiboom-Gill pulse train. The precision of these measurements is estimated to be about five percent, and the values for plain copper solutions agree to within five percent with the values reported by Morgan and Nolle.[8]

Since we are interested in producing a material with both T1 and T2 relaxation times equivalent to those of tissue, it is convenient to plot the relationship between T1 and T2 as concentration of the agarose and copper sulfate changes. Table 1 compares T1 and T2 values measured at 5 and 60 MHz for rabbit tissue with T1 and T2 values for plain agarose and copper solutions. Figure 1 is a T1–T2 plot of the 5 MHz data in Table 1. The plot of the 60 MHz data is similar. Figure 1 shows the extent of the mismatch of the relaxation times. Note that the values for the tissues fall between the solutions of pure agarose and pure copper sulfate.

Figure 2 is a log-log plot of T1 and T2 at 5 MHz for pure solutions of agarose and copper sulfate and of mixtures of agarose and copper sulfate. Dashed lines connect points of equal agarose or copper concentration. The upper right point corresponds to pure distilled deionized water. It can be seen that by selecting an appropriate percentage of agarose and concentration of copper sulfate a mixture with a T1 and T2 equivalent to a selected tissue can be produced. Again, a similar plot can be produced at 60 MHz. Note how T1 depends mostly on copper concentration and T2 depends mostly on agar concentration.

These graphs are not intended to imply a functional relationship between T1 and T2 but rather to act as nomograms allowing the selection of an appropriate

Table 1. Relaxation times in milliseconds of selected rabbit tissues and phantom materials. Means and standard deviations of three samples.

Material	5 MHz		60 MHz	
	T1	T2	T1	T2
Psoas Muscle	366 (19)	25 (2)	820 (36)	52 (6)
Renal Cortex	285 (37)	39 (8)	593 (9)	67 (10)
Renal Medulla	764 (25)	87 (26)	1180 (22)	123 (12)
Perirenal Fat	177 (36)	92 (12)	201 (5)	149 (10)
Blood	605 (50)	145 (9)	1140 (54)	250 (18)
$CuSO_4$ – 0.5mM	676 (12)	606 (12)	1469 (54)	1260 (58)
$CuSO_4$ – 1 mM	411 (8)	351 (11)	1002 (20)	970 (20)
$CuSO_4$ – 2 mM	206 (18)	181 (12)	564 (6)	557 (19)
$CuSO_4$ – 4 mM	116 (5)	100 (4)	320 (4)	298 (10)
Agarose 0.5% W/V	1481 (151)	240 (15)	2743 (71)	278 (43)
Agarose 1% W/V	1309 (106)	106 (26)	1790 (43)	89 (2)
Agarose 2% W/V	1122 (98)	56 (16)	1590 (50)	54 (4)
Agarose 4% W/V	1000 (92)	23 (9)	1390 (84)	27 (3)

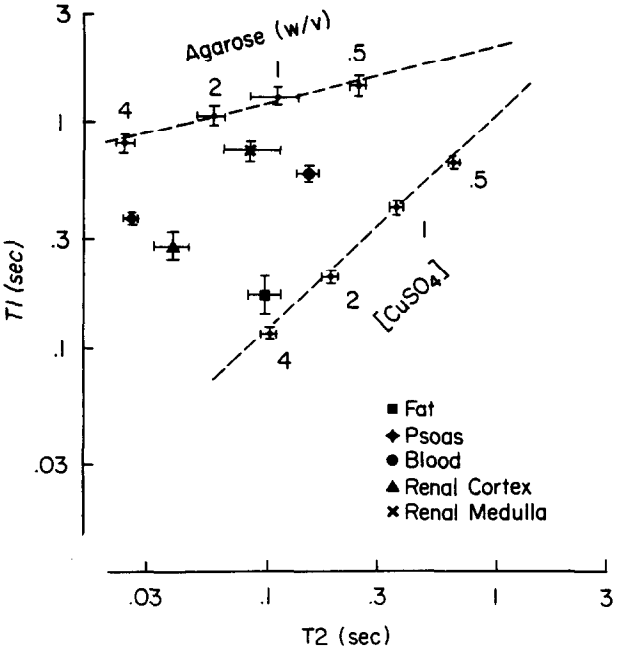

Fig. 1. T1 and T2 values for agarose in concentrations of 0.50 to 4.0% weight/volume; copper sulfate from 0.50 to 4.0 millimolar; and for selected rabbit tissues measured *in vitro*.

resulting from a 90° pulse followed by 180° pulses. The pulse interval was 8 or 12 milliseconds.

RESULTS AND DISCUSSION

To test the method, the relaxation times of air-saturated aqueous solutions of copper sulfate were measured. For all measurements, the temperature was 38° ± 2° C. The results are presented in Table I. T_1 and T_2 are equal for the copper solutions, and the relaxation times are inversely proportional to concentration except at the very lowest concentrations, where T_1 and T_2 become comparable to the relaxation times of water.

The progressive saturation data for the copper sulfate solutions are shown in Figure 1. Both peak height and peak area measurements gave the same result, but the measurement of peak height with negligible inhomogeneity was the most satisfactory. The peak height method in very inhomogeneous fields seems to be sensitive to the actual shape of the magnetic field, and if the inhomogeneity line width is not large enough, the apparent relaxation time will be high. The area method is time-consuming because the integral is recorded slowly. The relaxation time of water measured by this method (Table I) was low. The progressive saturation method seems to be susceptible to systematic errors, and not as reproducible as the direct method or the measurement of the line width. Also useful for comparison are the data on relaxation times in nickel-ammonia and nickel-cyanide solutions obtained in a recent study of the nickel-cyanide complex system (*12*). In this, T_1 was measured also by the direct method. From these results, it is apparent that the line width measurement gives the same result as the spin-echo technique. These nickel solutions exhibit different values for T_1 and T_2. This somewhat unusual phenomenon has been observed before (*3*).

Table I. Proton Spin Relaxation Times of Water and Aqueous Copper Sulfate Solutions

Concn., mM	$\sqrt{T_1T_2}$, sec. Prog. sat.	T_2, sec. Line width
Water	1.30	
2	0.53	0.58
4	0.33	0.27
16	0.090	0.090
50	0.037	0.029
100	0.021	0.016

ACKNOWLEDGMENT

We are grateful for many helpful discussions with Rolf W. Arndt.

LITERATURE CITED

(1) Abragam, A., "Principles of Nuclear Magnetism," p. 50, Clarendon Press, Oxford, England, 1961.
(2) Anderson, W., "NMR and EPR Spectroscopy," p. 180, Third Annual Workshop, Varian Association, Palo Alto, Calif., Pergamon Press, New York, 1960.
(3) Bernheim, R. A., Brown, T. H., Gutowsky, H. S., Woessner, D. E., *J. Chem. Phys.* **30,** 950 (1959).
(4) Bloembergen, N., Purcell, E. M., Pound, R. V., *Phys. Rev.* **73,** 679(1948).
(5) Carr, H. Y., Purcell, E. M., *Ibid.*, **94,** 630 (1954).
(6) Ernst, R., Varian Associates, Palo Alto, Calif., private communication, 1964.
(7) Luz, Z., Meiboom, S., *J. Chem. Phys.* **40,** 2686 (1964).
(8) Meiboom, S., Gill, D., *Rev. Sci. Instr.* **29,** 688 (1958).
(9) Nederbragt, G. W., Reilly, C. A., *J. Chem. Phys.* **24,** 1110 (1956).
(10) Pople, J. A., Schneider, W. G., Bernstein, H. J., "High Resolution Nuclear Magnetic Resonance," p. 82, McGraw-Hill, New York, 1959.
(11) Primas, H., *Helv. Phys. Acta* **31,** 17 (1958).
(12) Van Geet, A. L., Hume, D. N., *Inorg. Chem.* **3,** 523 (1964).
(13) Williams, R. B., *Ann. N. Y. Acad. Sci.* **70,** 890 (1958).

RECEIVED for review August 4, 1964. Resubmitted February 23, 1965. Accepted May 5, 1965. Work supported in part by the United States Atomic Energy Commission under Contract AT (30-1)-905.

Measurement of Proton Relaxation Times with a High Resolution Nuclear Magnetic Resonance Spectrometer

Direct Method

ANTHONY L. VAN GEET

Department of Chemistry, State University of New York at Buffalo, Buffalo, N. Y.

DAVID N. HUME

Department of Chemistry and Laboratory for Nuclear Science, Massachusetts Institute of Technology, Cambridge, Mass.

▶ **Details are given of an experimental technique whereby the proton relaxation time, T_1, may be measured with a high resolution nuclear magnetic resonance spectrometer, using the direct method. The method is best suited for relaxation times between 50 milliseconds and 25 seconds. A theoretical study of the method is made. The Bloch equations are solved under the simplifying assumption of negligible saturation ($\gamma H_1 \ll T_1^{-1}$). The result shows that a simple exponential signal recovery of time constant T_1 occurs only if the magnetic field is sufficiently inhomogeneous ($\Delta\gamma H_0 \gg T_2^{-1}$).**

PROTON nuclear magnetic resonance (NMR) spectra are widely used in structure determination and in qualitative and quantitative analysis of organic compounds. By comparison, much less attention has been given to relaxation time measurements (*13*) with this instrument. The transverse relaxation time, T_2, follows from the line width, of course, but relaxation times longer than about 1 second cannot be determined accurately in this way because of limited resolution.

This paper shows the longitudinal relaxation time, T_1, may readily be determined by the direct method (*11*).

In spite of its simplicity, the direct method has not found wide application (*3, 6*). In its simplest form, the sample is introduced into the magnetic field and one observes the signal growing in. It is not necessary to introduce the sample physically into the magnetic field. Instead, the sample may be saturated by the application of a sufficiently strong RF field, H_1, so $\gamma H_1 >> (T_1T_2)^{-1/2}$. When the amplitude of the RF field is suddenly reduced to a non-saturating value, the NMR signal (v-mode) recovers exponentially with a time constant which is essentially T_1.